J. Phys.: Condens. Matter **12** (2000) 3751–3765. Printed in the UK PII: S0953-8984(00)08074-7

Structural characterization of the $\beta \rightarrow \alpha$ superionic transition in Ag_2HgI_4 and Cu_2HgI_4

S Hull and D A Keen

The ISIS Facility, Rutherford Appleton Laboratory, Chilton, Didcot, Oxfordshire OX11 0QX, UK

E-mail: s.hull@rl.ac.uk and d.a.keen@rl.ac.uk

Received 23 September 1999

Abstract. The nature of the $\beta \rightarrow \alpha$ superionic transition in Ag_2HgI_4 and Cu_2HgI_4 has been investigated using temperature dependent powder neutron diffraction and impedance spectroscopy techniques. In the case of Ag_2HgI_4, the superionic $\beta \rightarrow \alpha$ transition occurs at $T_c = 326(2)$ K and is accompanied by a 50-fold increase in the ionic conductivity. In the Cu^+ analogue, which has a lower conductivity for a given temperature, the corresponding values are $T_c = 338(4)$ K and $\sigma_\alpha/\sigma_\beta \sim 6$. The ambient temperature crystal structures of the two compounds are different (space group $I\bar{4}$ for β-Ag_2HgI_4 and $I\bar{4}2m$ for β-Cu_2HgI_4) but, in contrast to the most recent study, the high temperature polymorphs are found to be isostructural (space group $F\bar{4}3m$). Possible explanations for the different behaviour of the ionic conductivity of the two compounds are given.

1. Introduction

On increasing temperature, the binary compounds silver iodide (AgI) and copper iodide (CuI) undergo first-order transitions to the superionic state at $T = 420$ K and $T = 642$ K, respectively (see [1] and references therein). The superionic phases, labelled α-AgI and α-CuI, are characterized by high values of the ionic conductivity σ, which are comparable to the molten state ($\sigma \sim 0.1$-1 Ω^{-1} cm^{-1}). In the generally accepted structural model, the monovalent cations undergo rapid hops between the tetrahedral interstices formed by an essentially rigid anion sublattice, which is body centred cubic (b.c.c.) in α-AgI [2] and face centred cubic (f.c.c.) in α-CuI [3]. Potential technological applications of Ag^+ and Cu^+ based superionics in solid state battery and chemical sensor devices has motivated considerable research aimed at preparing compounds with a superionic transition closer to ambient temperature. The principal method adopted is chemical doping. In the case of AgI, partial replacement of the (immobile) anions leads to compounds such as the 'anti-perovskite' structured Ag_3SI [4], whilst isovalent and aliovalent doping of the cation sites produces systems such as Ag_4RbI_5 [5] and Ag_2HgI_4, respectively. Whilst these doping strategies have successfully lowered the transition temperature, the structural mechanisms by which this is achieved remain unclear (for details, see Chandra [1]). There are three possibilities:

(i) The dopant cations act simply produce vacant sites for mobile cations (i.e. $2Ag^+ \rightarrow Hg^{2+} + \square$ in Ag_2HgI_4, where $\square$ denotes a vacancy).
(ii) The dopant cations act as 'structural modifiers', forcing the immobile anion sublattice to adopt configurations which favour rapid cation diffusion.
(iii) The dopant cations are themselves mobile and so contribute directly to the high ionic conductivity within the superionic phase.

0953-8984/00/163751+15$30.00 © 2000 IOP Publishing Ltd

As discussed more fully in the following section, this debate has been most active in the case of Ag_2HgI_4 and its copper analogue Cu_2HgI_4. Both undergo discontinuous superionic transitions (type I in the notation of Boyce and Huberman [6]) at $T \approx 323$ K and $T \approx 342$ K, respectively. Indeed, T_c falls to ~306 K at the eutectic concentration $x \sim 1.14$ in $(Ag_xCu_{2-x})HgI_4$, with the room temperature ionic conductivity $\sigma_{293\ K} = 2 \times 10^{-5}\ \Omega^{-1}\ cm^{-1}$ [7, 8]. The $\beta \rightarrow \alpha$ transition is accompanied by abrupt colour changes from yellow to orange in Ag_2HgI_4 and red to dark maroon in Cu_2HgI_4. However, there is relatively poor agreement within the literature concerning the exact values of σ below and above the transition [9–15]. In general, σ jumps from $\sim 10^{-5}\ \Omega^{-1}\ cm^{-1}$ to $\sim 10^{-3}\ \Omega^{-1}\ cm^{-1}$ in Ag_2HgI_4 and from $\sim 10^{-6}\ \Omega^{-1}\ cm^{-1}$ to $\sim 10^{-5}\ \Omega^{-1}\ cm^{-1}$ in Cu_2HgI_4. Most significantly, superionic α-Cu_2HgI_4 is a rather poorer conductor than its Ag^+ counterpart. This fact, coupled with the possibility of unwanted electronic conductivity due to oxidation of mobile Cu^+ to Cu^{2+}, is a serious barrier to the use of Cu_2HgI_4 in commercial devices, despite the obvious cost advantages over Ag_2HgI_4. The aim of this work is to establish the differences in structural behaviour between Ag_2HgI_4 and Cu_2HgI_4 and resolve discrepancies present in the existing literature.

2. The crystal structures of Ag_2HgI_4 and Cu_2HgI_4

The binary compounds CuI and AgI both adopt the cubic zincblende structure (labelled the γ phases, space group $F\bar{4}3m$) at ambient pressure and temperature, though the latter usually exists as a two phase mixture containing a fraction of the hexagonal equivalent wurtzite β phase [16]. The first diffraction studies of the ternary compounds Ag_2HgI_4 and Cu_2HgI_4 in their room temperature (β) phases by Ketelaar [17] described them as isostructural, with a pseudo-cubic tetragonal unit cell (with $c_{tet} \sim a_{tet}$) in space group $P\bar{4}2m$. The ionic arrangement closely resembled zincblende, with a slightly distorted f.c.c. I^- sublattice and the $2 \times Ag^+$ and $1 \times Hg^{2+}$ ordered over the four tetrahedral sites which are occupied in, for example, γ-AgI. Subsequent x-ray diffraction measurements by Hahn [18] showed that the Ag^+ and Cu^+ counterparts possess different structures, though both have doubled zincblende unit cells along one of the 'cubic' axes such that $c_{tet} \sim 2a_{tet}$. Both structures can be derived from chalcopyrite, $CuFeS_2$ (i.e. $Cu_2Fe_2S_4$) by distributing the $4 \times M^+$, $2 \times Hg^{2+}$ and $2 \times \square$ in different ways over the eight cation sites. Their space groups are $I\bar{4}$ (β-Ag_2HgI_4) and $I\bar{4}2m$ (β-Cu_2HgI_4) and the full crystallographic description of the two alternatives is given in table 1. As illustrated schematically in figure 1, the vacant cation sites in β-Ag_2HgI_4 are occupied by monovalent cations in β-Cu_2HgI_4, and vice versa. The crystal structures of β-Ag_2HgI_4 and β-Cu_2HgI_4 were subsequently confirmed by Brownall *et al* [19] and Berthold and Kasse [20], respectively. The former showed that single crystals of the β phase generally exist as multidomain twinned samples, with the $[001]_{tet}$ direction aligned randomly along one of the three principal pseudo-cubic axes.

The structures of the high temperature superionic phases α-Ag_2HgI_4 and α-Cu_2HgI_4 were reported by Ketelaar [21] to be the same disordered cubic zincblende type, with the I^- forming an ideal f.c.c. sublattice and the $2 \times M^+$, $1 \times Hg^{2+}$ and $1 \times \square$ randomly distributed over the four tetrahedral (zincblende) sites. This assignment was subsequently confirmed for α-Ag_2HgI_4 by Kasper and Brownall [22] and for β-Cu_2HgI_4 by Berthold and Kasse [20]. The former showed that both the anions and cations undergo extensive anharmonic thermal vibrations in the $\langle 111 \rangle$ directions, such that the fourfold sites at $\frac{1}{4}, \frac{1}{4}, \frac{1}{4}$ etc can be modelled as 16 'split-site' positions at x, x, x etc with $x \sim 0.275$ and with a mean occupancy of $\frac{1}{4}$. This model is supported by far-infrared studies indicating significant anharmonic thermal vibrations of Ag^+ [9] but has been contested by Hibma *et al* [23], who suggest that the diffraction data are in fact modelling local

Table 1. A schematic diagram to illustrate the crystallographic relationship between the structures of β-Ag_2HgI_4 [19] and β-Cu_2HgI_4 [25] with that of chalcopyrite. □ denotes a cation vacancy.

β-Ag_2HgI_4	Chalcopyrite	β-Cu_2HgI_4
$I\bar{4}$	$I\bar{4}2d$	$I\bar{4}2m$
$Ag_2Hg\square I_4$	$A_2B_2X_4$	$Cu_2Hg\square I_4$
I^- in 8(g) x, y, z $x \sim \frac{1}{4}, y \sim \frac{1}{4}, z \sim \frac{1}{8}$	X in 8(d) $x, \frac{1}{4}, \frac{1}{8}$ $x \sim \frac{1}{4}$	I^- in 8(i) x, x, z $x \sim \frac{1}{4}, z \sim \frac{1}{8}$
Hg^{2+} in 2(a) 0, 0, 0	A in 4(a) 0, 0, 0	Hg^{2+} in 2(a) 0, 0, 0
$Ag2^+$ in 2(c) 0, $\frac{1}{2}$, $\frac{1}{4}$		Cu^+ in 4(d) 0, $\frac{1}{2}$, $\frac{1}{4}$
□ in 2(d) 0, $\frac{1}{2}$, $\frac{3}{4}$	B in 4(b) 0, 0, $\frac{1}{2}$	
$Ag1^+$ in 2(b) 0, 0, $\frac{1}{2}$		□ in 2(b) 0, 0, $\frac{1}{2}$

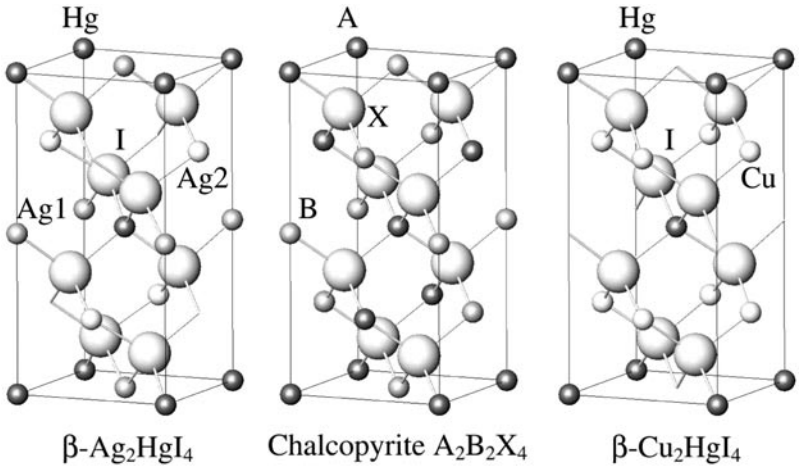

Figure 1. The crystal structures of β-Ag_2HgI_4 (left) and β-Cu_2HgI_4 (right) illustrating their relationship to the chalcopyrite structure (centre).

'static' displacements of the ions as each 'sees' an extremely complex surrounding environment of unlike ions. Their x-ray diffraction studies of single crystal α-Ag_2HgI_4 showed extensive disc-shaped features in the diffuse scattering, interpreted as local order of the Hg^{2+}, which avoid nearest neighbour contacts (as observed in ordered β-Ag_2HgI_4). This model is supported by reports of the relatively low transference number of Hg^{2+} ($t_{Hg} = 0.06$ [24]). However, the most recent high temperature x-ray diffraction study of α-Cu_2HgI_4 [25] suggested that the high temperature phase is tetragonal (though with $c_{tet} = 2a_{tet}$ within experimental error). The space group ($I\bar{4}2m$) is the same as the low temperature β phase and the superionic $\beta \rightarrow \alpha$ transition merely involves a disordering of the $2 \times Hg^{2+}$ and $2 \times \square$. The $4 \times Cu^+$ remain localized on the same sites as β-Cu_2HgI_4, such that α-Cu_2HgI_4 is predominantly an Hg^{2+} conductor. Clearly, this provides a possible explanation for the lower conductivity of α-Cu_2HgI_4 compared to α-Ag_2HgI_4.

This paper reports a systematic study of Ag_2HgI_4 and Cu_2HgI_4 in their β and α forms using neutron powder diffraction and impedance spectroscopy. These neutron measurements

have been used to resolve the structural ambiguities that have arisen from various earlier x-ray diffraction studies. Despite the high neutron absorption of Hg and Ag, good quality diffraction data have been measured to small d spacings to yield precise structural models. In addition, samples were encapsulated under vacuum to reduce problems of sample degradation and identical samples were used for the impedance spectroscopy measurements.

3. Experiment

The samples of Ag_2HgI_4 and Cu_2HgI_4 used in this study were supplied by the Cerac Chemical Co. and of stated purity 99.5%. Neutron diffraction data confirmed the absence of any additional impurity phases in either sample. Two-terminal measurements of the ionic conductivity were performed using pelleted samples of ∼7 mm diameter and ∼5 mm length and graphite contacts. The proximity of the superionic transitions to ambient temperature required that measurements be made at elevated temperatures in a furnace and to low temperatures in a closed cycle refrigerator. Details of both devices can be found elsewhere [26]. However, the structural behaviour of both compounds below ∼250 K is reported to be extremely complex, with reports of numerous phase transitions [27, 28] and data were not collected below this temperature. A PC controlled Solartron S1260 Frequency Response Analyser determined the conventional Z-Z' impedance plot over the frequency range from 0.1 Hz to 10 MHz. The real component of the sample impedance Z_S was determined using the program IMMFIT [26].

Diffraction experiments were performed using the Polaris powder diffractometer at the ISIS facility, UK [29]. The samples were encapsulated under vacuum inside silica tubes, of approximate wall thickness 0.5 mm, and heated inside a furnace constructed from a vanadium resistive heating element and heat shields. Data were collected using detector banks which cover the scattering angles $85^\circ < \pm 2\theta < 95^\circ$ and provide data over the d-spacing range $\sim 0.3 < d$ (Å) $<\sim 4.3$ with a resolution $\Delta d/d \sim 6 \times 10^{-3}$. Rietveld profile refinement used the program TF12LS [30], which is based on the Cambridge Crystallographic Subroutine Library [31]. Coherent scattering lengths of $b_{Ag} = 5.922$ fm, $b_{Cu} = 7.718$ fm, $b_{Hg} = 12.692$ fm and $b_I = 5.28$ fm were used [32]. In assessing the relative quality of fits to the experimental data using different structural models the usual χ^2 statistic is used, defined by

$$\chi^2 = \sum_{N_d} \frac{(I_{obs} - I_{calc})^2}{(\sigma I_{obs})^2} / (N_d - N_p).$$

N_d is the number of data points used in the fit and N_p is the number of fitted parameters. I_{obs} and I_{calc} are the observed and calculated intensities, respectively, and σI_{obs} is the estimated standard deviation on I_{obs}, derived from the counting statistics.

4. Results

4.1. Impedance spectroscopy

The results of the measurements of the ionic conductivity of Ag_2HgI_4 and Cu_2HgI_4 are shown in figure 2. The general behaviour is in broad agreement with that published previously [9–15] though, as discussed in section 2, there is some variability in the precise levels of σ in the earlier reports. The $\beta \rightarrow \alpha$ phase transition is clearly seen in both samples and occurs at 326(2) and 338(4) K in Ag_2HgI_4 and Cu_2HgI_4, respectively. The discontinuous jump in conductivity is larger in Ag_2HgI_4 ($\sigma_\alpha/\sigma_\beta \approx 50$) than Cu_2HgI_4 ($\sigma_\alpha/\sigma_\beta \approx 6$), though σ rises more rapidly above the transition in the latter material.

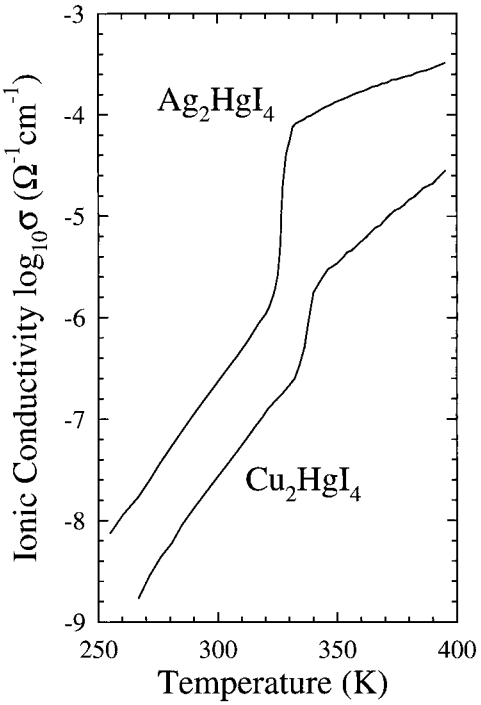

Figure 2. The variation of the ionic conductivity σ of Ag_2HgI_4 and Cu_2HgI_4 with temperature, illustrating the first-order $\beta \rightarrow \alpha$ superionic transitions at $T = 326(2)$ K and $T = 338(4)$ K, respectively.

The measurements of the ionic conductivity presented in figure 2 were performed under dynamic vacuum of $\sim 10^{-2}$ Pa. Those samples cooled from $\sim$400 K showed reproducible behaviour on subsequent reheating and no evidence of degradation. However, samples taken to temperatures significantly above 400 K underwent a loss of HgI and, as a result, no measurements above this temperature are reported here. These results do not constitute a definitive determination of the absolute values of the ionic conductivity of Ag_2HgI_4 and Cu_2HgI_4, but rather serve to demonstrate that the samples used in the neutron diffraction measurements display ionic conductivities consistent with previous measurements. It is, however, believed that with similarly prepared samples and an identical measuring method, the relative values of σ are reproducible and reliable.

4.2. Neutron diffraction: the ambient temperature β phases

The diffraction patterns for the 'non-superionic' β phases of Ag_2HgI_4 and Cu_2HgI_4 collected at room temperature were initially fitted using the structures which have most recently been reported within the literature, in space groups $I\bar{4}$ and $I\bar{4}2m$, respectively [19, 25]. In both cases these structural models gave excellent fits to the experimental data, with χ^2 values of 1.97 and 2.05 for β-Ag_2HgI_4 and β-Cu_2HgI_4, respectively. The quality of these fits is illustrated in figures 3 and 4 and the structural parameters obtained are listed in tables 2 and 3. Attempts to fit the data for β-Ag_2HgI_4 using the structural model for its Cu^+ analogue (and vice versa) produced significantly poorer fits and we therefore conclude that the two compounds are not isostructural under ambient conditions. Indeed, their tetragonal c/a ratios are different, being

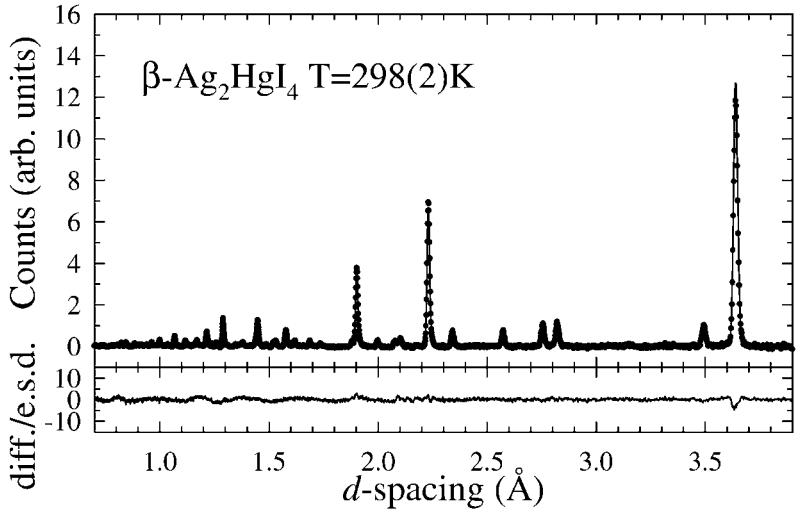

Figure 3. Fit to the neutron diffraction data collected from β-Ag_2HgI_4 at $T = 298(2)$ K. The dots are the experimental data points and the solid line is the calculated profile using the structural parameters listed in table 2. The lower trace represents the difference (observed minus calculated) divided by the estimated standard deviation on the points.

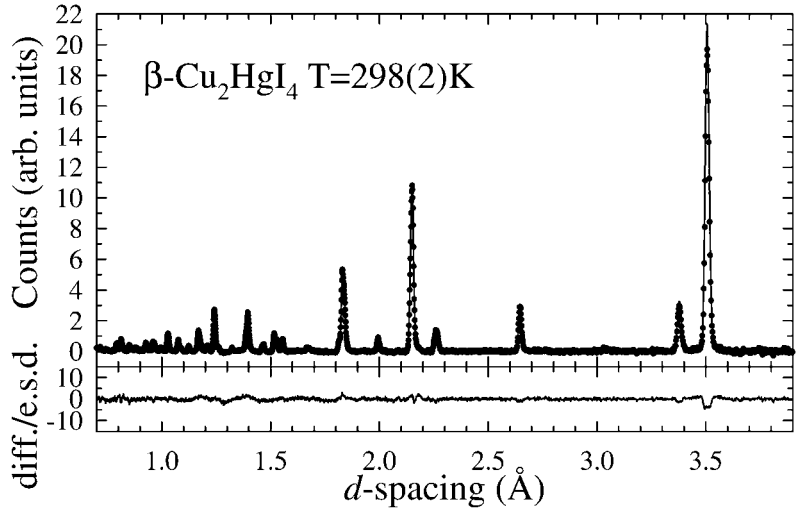

Figure 4. Fit to the neutron diffraction data collected from β-Cu_2HgI_4 at $T = 298(2)$ K. The dots are the experimental data points and the solid line is the calculated profile using the structural parameters listed in table 3. The lower trace represents the difference (observed minus calculated) divided by the estimated standard deviation on the points.

slightly greater than the ideal value of 2 in β-Cu_2HgI_4 and very marginally lower than 2 in β-Ag_2HgI_4. On increasing temperature the tetragonal distortion decreases in both compounds (see figure 5).

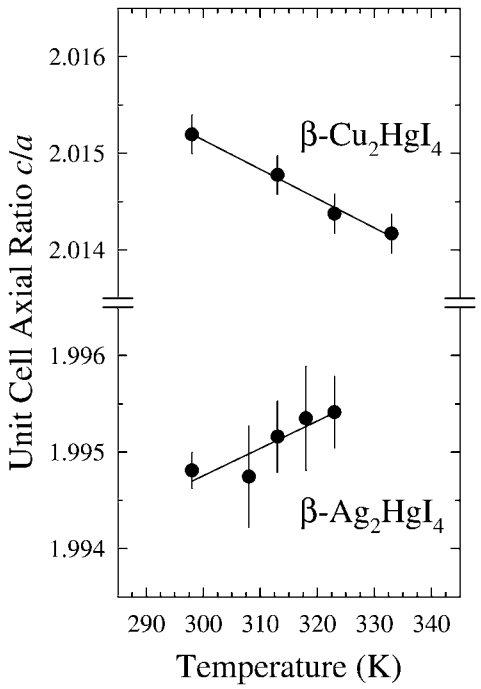

Figure 5. The variation of the tetragonal c/a axial ratio with temperature for β-Ag_2HgI_4 and β-Cu_2HgI_4.

4.3. Neutron diffraction: the superionic α phases

The presentation of the neutron diffraction results for the high temperature superionic α phases of Ag_2HgI_4 and Cu_2HgI_4 will consider a total of four datasets, collected for relatively long times (10–12 hours) in order to obtain the counting statistics necessary to reliably differentiate between different, though closely related, structural models. These are α-Ag_2HgI_4 ($T = 338(2)$ K and $T = 398(2)$ K) and α-Cu_2HgI_4 ($T = 363(2)$ K and $T = 473(3)$ K). In view of the conflicting reports given in the literature concerning the structures of these two compounds within their high temperature α phases, we adopt a rather general approach and fit a series of structural models to the data and determine the correct description using the χ^2 statistic defined in section 3.

The structural models used to fit the four diffraction datasets are labelled I to IV and are summarized in table 4. Model I addresses the initial question of the correct unit cell description and space group assignment. In particular, it aims to resolve whether, on the basis of the observed Bragg peak positions, the unit cell is cubic (with $a \approx 6.3$ Å for Ag_2HgI_4 and $a \approx 6.1$ Å for Cu_2HgI_4) or tetragonal (with $c \approx 2a$). These correspond to models Ia and Ib, respectively. The variable parameters during the fitting procedure are five polynomial coefficients describing the background scattering, the unit cell constant(s), a Gaussian width parameter describing the sample contribution to the Bragg peak shape and intensities of all the Bragg peaks consistent with the unit cell. The space groups are chosen to be $Pm\bar{3}m$ (model Ia) and $P4/mmm$ (model Ib) because these impose no systematic absences on reflections. As such, model I does not impose (or provide) any direct structural information concerning the ionic positions. In the case of the two superionic phases, a cubic unit cell appears to be the best

Table 2. A summary of results from the Rietveld refinements of the diffraction data for Ag_2HgI_4.

Phase	β	α	
Space group	$I\bar{4}$	$F\bar{4}3m$	
Temperature	$T = 298(2)$ K	$T = 338(2)$ K	$T = 398(2)$ K
Unit cell constants	$a = 6.3194(3)$ Å $c = 12.606(1)$ Å $c/a = 1.9948(2)$	$a = 6.3337(1)$ Å	$a = 6.3395(1)$ Å
Formula units in unit cell	$Z = 2$	$Z = 1$	$Z = 1$
Unit cell volume	$V/Z = 251.71(2)$ Å^3	$V/Z = 254.081(4)$ Å^3	$V/Z = 254.780(4)$ Å^3
I^-	8(g) at x_I, y_I, z_I $x_I = 0.271(1)$ $y_I = 0.229(2)$ $z_I = 0.135(1)$ $B_I = 2.1(2)$ Å^2	4(c) at $\frac{1}{4}, \frac{1}{4}, \frac{1}{4}$ $B_I = 4.8(3)$ Å^2	4(c) at $\frac{1}{4}, \frac{1}{4}, \frac{1}{4}$ $B_I = 6.4(5)$ Å^2
Hg^{2+}	2(a) at 0, 0, 0 $B_{Hg} = 2.5(2)$ Å^2	4(a) at 0, 0, 0 $B_{Hg} = 4.4(2)$ Å^2 occupancy= $\frac{1}{4}$	4(a) at 0, 0, 0 $B_{Hg} = 5.0(3)$ Å^2 occupancy= $\frac{1}{4}$
Ag^+	2(b) at 0, 0, $\frac{1}{2}$ $B_{Ag1} = 1.8(3)$ Å^2 2(c) at 0, $\frac{1}{2}, \frac{1}{4}$ $B_{Ag2} = 2.3(3)$ Å^2	4(a) at 0, 0, 0 $B_{Ag} = B_{Hg}$ occupancy= $\frac{1}{2}$	4(a) at 0, 0, 0 $B_{Ag} = B_{Hg}$ occupancy= $\frac{1}{2}$
Weighted profile R-factor	$R_w = 1.43$	$R_w = 1.16$	$R_w = 1.11$
Expected R-factor	$R_{\text{exp}} = 1.02$	$R_{\text{exp}} = 0.45$	$R_{\text{exp}} = 0.45$
Goodness of fit	$\chi^2 = 1.97$	$\chi^2 = 6.64$	$\chi^2 = 6.08$
Number of data points	$N_d = 3291$	$N_d = 3291$	$N_d = 3291$
Number of Bragg peaks	$N_p = 804$	$N_p = 112$	$N_p = 112$

description, with no evidence of broadening of peaks such as $00l : l = 2n$ and no additional reflections at positions disallowed in the cubic setting. In general, fits using the tetragonal unit cell of model Ib were unstable and the χ^2 value failed to converge satisfactorily. The reflection conditions for the cubic unit cell are hkl with h, k, l, all odd or all even; $0kl$ with k and l even; hhl with $h + l$ even and $00l$ with l even. These are consistent with several space groups, including $F\bar{4}3m$ proposed for the high temperature superionic phases (α-Ag_2HgI_4 and α-Cu_2HgI_4) and also with its centrosymmetric counterpart $Fm\bar{3}m$. We should note that the values of χ^2 obtained using model Ia (see table 5) are representative of the 'best-fit' possible and can be used to judge the quality of the subsequent fits which impose structural constraints during the fitting procedure.

Model II represents the situation of fully ordered cations, with the $4 \times Ag^+/Cu^+$ and $2 \times Hg^{2+}$ arranged over the eight tetrahedral sites in space groups $I\bar{4}$ and $I\bar{4}2m$, both with $c = 2a$ (see figure 1). As discussed in section 4.2, the former provides the best fit to the data for β-Ag_2HgI_4 at ambient temperature whilst the latter successfully describes the structure of β-Cu_2HgI_4. However, the four high temperature datasets for α-Ag_2HgI_4 and α-Cu_2HgI_4 are not well fitted using model II, indicating that some, or all, of the cation species are disordered. Model III allows partial disorder, with either the Ag^+/Cu^+ or the Hg^{2+} distributed over the sites occupied within the β phases and the vacant tetrahedral positions. With reference to figure 1, it is clear that the effect of distributing the Ag^+/Cu^+ over the occupied and vacant sites within the two different β phase structures will produce a very similar structural model, with the exception that the I^- occupy general 8(g) positions at x, y, z in $I\bar{4}$ symmetry and special 8(i) x, x, z ones

Table 3. A summary of results from the Rietveld refinements of the diffraction data for Cu_2HgI_4.

Phase	β	α	
Space group	$I\bar{4}2m$	$F\bar{4}3m$	
Temperature	$T = 298(2)$ K	$T = 363(2)$ K	$T = 473(3)$ K
Unit cell constants	$a = 6.0672(1)$ Å $c = 12.2266(4)$ Å $c/a = 2.0152(1)$	$a = 6.1086(1)$ Å	$a = 6.1285(1)$ Å
Formula units in unit cell	$Z = 2$	$Z = 1$	$Z = 1$
Unit cell volume	$V/Z = 225.036(8)$ Å^3	$V/Z = 227.942(4)$ Å^3	$V/Z = 230.177(4)$ Å^3
I^-	8(i) at x_I, x_I, z_I $x_I = 0.2678(7)$ $z_I = 0.1240(11)$ $B_I = 1.0(1)$ Å^2	4(c) at $\frac{1}{4}, \frac{1}{4}, \frac{1}{4}$ $B_I = 2.8(1)$ Å^2	4(c) at $\frac{1}{4}, \frac{1}{4}, \frac{1}{4}$ $B_I = 4.3(1)$ Å^2
Hg^{2+}	2(a) at 0, 0, 0 $B_{Hg} = 1.4(1)$ Å^2	4(a) at 0, 0, 0 $B_{Hg} = 2.32(7)$ Å^2 occupancy= $\frac{1}{4}$	4(a) at 0, 0, 0 $B_{Hg} = 3.22(7)$ Å^2 occupancy= $\frac{1}{4}$
Cu^+	4(d) at 0, $\frac{1}{2}, \frac{1}{4}$ $B_{Cu} = 0.8(2)$ Å^2	4(a) at 0, 0, 0 $B_{Cu} = B_{Hg}$ occupancy= $\frac{1}{2}$	4(a) at 0, 0, 0 $B_{Cu} = B_{Hg}$ occupancy= $\frac{1}{2}$
Weighted profile R-factor	$R_w = 1.96$	$R_w = 1.35$	$R_w = 1.20$
Expected R-factor	$R_{\text{exp}} = 1.37$	$R_{\text{exp}} = 0.45$	$R_{\text{exp}} = 0.5$
Goodness of fit	$\chi^2 = 2.05$	$\chi^2 = 9.00$	$\chi^2 = 4.94$
Number of data points	$N_d = 3291$	$N_d = 3291$	$N_d = 3291$
Number of Bragg peaks	$N_p = 792$	$N_p = 101$	$N_p = 101$

Table 4. A summary of the possible structural models used to interpret the diffraction data for the superionic phases α-Ag_2HgI_4 and α-Cu_2HgI_4.

			Ionic positions		
Model	Description	Space group	I^-	Hg^{2+}	Ag^+/Cu^+
Ia	Model independent (tetragonal)	$P4mmm$	—	—	—
Ib	Model independent (cubic)	$Pm\bar{3}m$	—	—	—
IIa	Cation ordered ('β-Ag_2HgI_4' [19])	$I\bar{4}$	8(g)	2(a)	2(b)+29c)
IIb	Cation ordered ('β-Cu_2HgI_4' [25])	$I\bar{4}2m$	8(i)	2(a)	4(d)
IIIa	Ag^+/Cu^+ disorder only	$I\bar{4}$	8(g)	2(s)	2(b)+2(c)+2(d) occ = $\frac{1}{2}$
IIIb	Hg^{2+} disorder only	$I\bar{4}$	8(g)	2(a)+2(d)	2(b)+2(c)
IIIc	Hg^{2+} disorder only	$I\bar{4}2m$	8(i)	2(a)+2(b) occ = $\frac{1}{2}$	4(d)
IVa	$Ag^+/Cu^+ + Hg^{2+}$ disorder (zincblende)	$F\bar{4}3m$	4(a)	4(c) occ = $\frac{3}{4}$	4(c) occ = $\frac{3}{4}$
Ivb	$Ag^+/Cu^+ + Hg^{2+}$ disorder ('α-CuI')	$Fm\bar{3}m$	4(a)	8(c) occ = $\frac{3}{8}$	8(c) occ = $\frac{3}{8}$

in $I\bar{4}2m$. We therefore consider only the former and label this model IIIa. In the case of immobile Ag^+/Cu^+ and disordered Hg^{2+}, the β-Ag_2HgI_4 and β-Cu_2HgI_4 arrangements lead to two distinct structural models. These are labelled IIIb and IIIc, respectively (see table 4).

Table 5. The values of the goodness-of-fit χ^2 statistic obtained by fitting the diffraction data for α-Ag_2HgI_4 at $T = 338(2)$ K and $T = 398(2)$ K and for α-Cu_2HgI_4 at $T = 363(2)$ K and $T = 473(3)$ K using the structural models listed in table 4. × indicates that the least-squares fit failed to converge satisfactorily.

Phase	T	Ia	Ib	IIa	II	IIIa	IIIb	IIIc	IVa	IVb
β-Ag_2HgI_4	338(2)	5.92	×	10.31	10.81	6.92	7.31	7.50	6.64	7.21
	398(2)	5.11	×	11.02	10.71	6.31	7.65	7.42	6.08	7.03
β-Cu_2HgI_4	363(2)	7.82	×	14.33	14.20	9.22	10.14	10.23	9.00	10.14
	473(3)	4.04	4.11	10.11	11.33	5.10	7.02	8.14	4.94	5.33

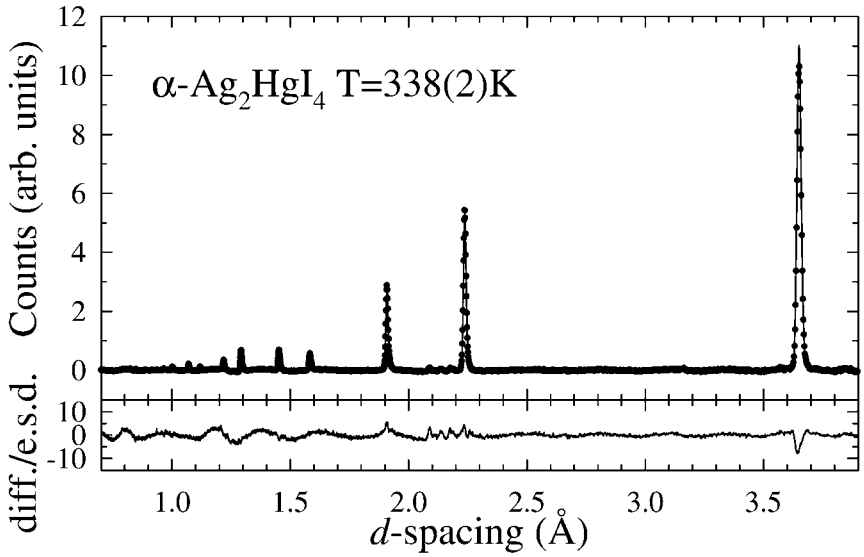

Figure 6. Fit to the neutron diffraction data collected from α-Ag_2HgI_4 at $T = 338(2)$ K. The dots are the experimental data points and the solid line is the calculated profile using the structural parameters listed in table 2. The lower trace represents the difference (observed minus calculated) divided by the estimated standard deviation on the points.

Model IV allows complete disorder of both the cation species. Model IVa adopts cubic space group $F\bar{4}3m$ and distributes the $2 \times Ag^+/Cu^+$ and $1 \times Hg^{2+}$ over the four tetrahedral 4(c) sites that would be fully occupied in a zincblende structured compound. With reference to table 5, it is clear that this structural description provides a better fit to the diffraction data for both α-Ag_2HgI_4 and α-Cu_2HgI_4 than the partially disordered cases considered in model III (and proposed for the case of α-Cu_2HgI_4 by recent x-ray diffraction work [25]). Although the improvement of the χ^2 values of model IVa over the χ^2 values of model IIIa are small, they are significant when compared to the 'best possible' values provided by model Ia in which no structural information is imposed. Furthermore, since there is no evidence of a tetragonal distortion of the unit cell (even with data collected at improved resolution using detectors situated at higher scattering angles), the cubic model IVa is preferred. The results are listed in tables 2 and 3 and the fits to the diffraction data collected from α-Ag_2HgI_4 at $T = 338(2)$ K and α-Cu_2HgI_4 at $T = 362(2)$ K are illustrated in figures 6 and 7, respectively.

A subsequent fit to the data was attempted (model IVb) in which the three cations are allowed to randomly occupy all eight of the tetrahedral interstices formed by the immobile I^-

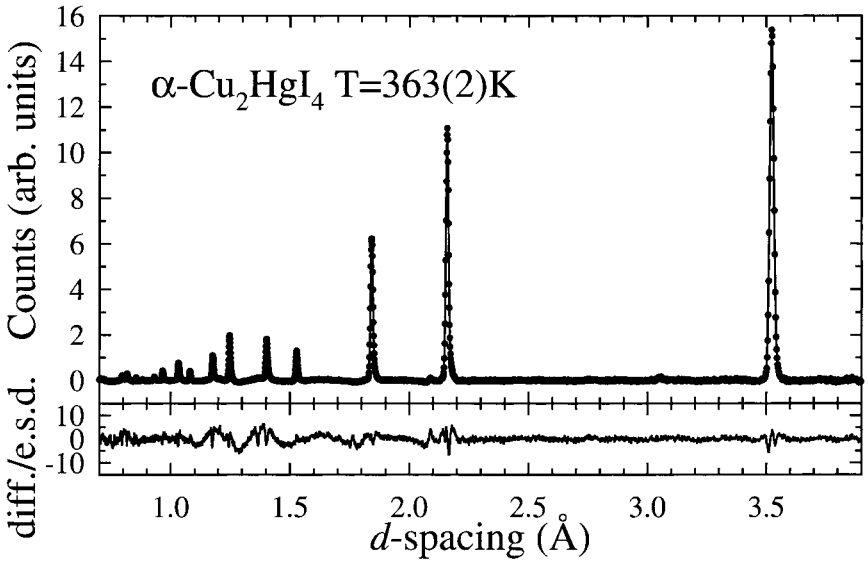

Figure 7. Fit to the neutron diffraction data collected from α-Cu_2HgI_4 at $T = 363(2)$ K. The dots are the experimental data points and the solid line is the calculated profile using the structural parameters listed in table 3. The lower trace represents the difference (observed minus calculated) divided by the estimated standard deviation on the points.

sublattice, rather than only the four that would be occupied in a zincblende-type arrangement. This corresponds to space group $Fm\bar{3}m$ which, we recall, cannot be distinguished from $F\bar{4}3m$ on the basis of the systematic peak absences. This disordering process occurs during the transition from the zincblende structured γ phase to the superionic α phase in CuI, with a gradual redistribution of Cu^+ ions over all the tetrahedral holes [3]. (Although the situation is complicated by the presence of the intervening hexagonal β phase over a narrow temperature range which interrupts the 'second-order' $\gamma \rightarrow \alpha$ transition [33].) As a result, a tendency towards this arrangement might be expected on increasing temperature. However, the poorer χ^2 values obtained using model IVb do not support such a suggestion. Similarly, trial refinements found no evidence of slight displacements of the cations away from the tetrahedral positions in $\langle 111 \rangle$ directions (to model the anharmonic thermal vibrations [22]) and attempts to include a fraction of Ag^+/Cu^+ on octahedral positions failed to converge.

5. Discussion

The structural information concerning the two ambient temperature β phases of Ag_2HgI_4 and Cu_2HgI_4 presented in this work are in accord with the most recent published structures in the literature [19, 25]. In particular, the two compounds are not isostructural, with different arrangements of the cation vacancies over the available tetrahedral sites which are fully occupied in a zincblende type structure. In the case of β-Ag_2HgI_4, this leads to two crystallographically distinct Ag^+ sites. The anion environment around each cation (Ag1, Ag2 and Hg) is very close to ideal tetrahedral and the nearest neighbour cation shell is essentially the same, with eight cations and four vacancies. However, the next nearest neighbour shell of six are different, there being two vacancies in the case of Ag2 and only one for Ag1 and Hg. This presumably explains the somewhat higher values of isotropic thermal vibration parameter for the former (see table 2).

It is generally accepted that superionic phases with a b.c.c. sublattice of immobile ions possess higher values of ionic conductivity than those with an f.c.c. sublattice, as illustrated by the comparison of α-AgI with α-CuI [6]. This can simply be explained by the preference of Cu^+ and Ag^+ to diffuse between interstices which possess tetrahedral co-ordination and a higher number of such sites/anion in b.c.c. (six) than f.c.c. (two). In comparison with α-CuI, the two superionic phases investigated in this work are formed at lower temperatures but have ionic conductivities $\sim 10^3$ times lower. This is somewhat surprising, since they adopt an f.c.c. I^- sublattice and might then be expected to show somewhat similar behaviour to α-CuI. However, the diffraction studies performed in this work show clearly that the mobile cations in both α-Ag_2HgI_4 and α-Cu_2HgI_4 only diffuse between a subset of the tetrahedral interstices and the number of available sites per cation is then only $\frac{4}{3}$, rather than two as in the case of α-CuI. Clearly, this feature is related to the presence of the large divalent species, which presumably avoid close Hg^{2+}-Hg^{2+} contact during the diffusion process. Such a tendency has been suggested to account for the strongly anisotropic nature of the diffuse scattering observed in single crystal x-ray diffraction studies of α-Ag_2HgI_4 [23].

In contrast to the most recent studies [25], we find no significant structural difference between the superionic α phases of Ag_2HgI_4 and Cu_2HgI_4, with disorder of both Ag^+/Cu^+ and Hg^{2+}. Since Cu^+ is smaller than Ag^+ ($r_{Cu^+} = 0.60$ Å compared to $r_{Ag^+} = 1.10$ Å [34]), one might intuitively expect α-Cu_2HgI_4 to have a higher ionic conductivity than α-Ag_2HgI_4, since the cations must hop through the 'gaps' in the sublattice formed by the immobile anions. However, measurements of the ionic conductivity indicate that in the Ag^+ compound it is $\sim 40\times$ higher than in the Cu^+ compound at 350 K (see figure 2). A possible explanation of this fact lies in the lower polarizability of Cu^+, so that Ag^+ may be better able to 'deform' whilst hopping through the triangular faces formed by the f.c.c. I^- sublattice. Alternatively, the diffusion between tetrahedral sites may occur via the octahedral positions though, as discussed in section 4.3, there is no evidence in the analysis of the diffraction data to suggest that these sites are stable minima. If so, this behaviour would favour the Ag^+ compound because its bonding has a more ionic character (with a higher Phillips' ionicity $f_{AgI} = 0.770$ and $f_{CuI} = 0.692$ [35]). Indirect support for this motion is provided by the structural behaviour of AgI and CuI under hydrostatic pressures, since the former adopts the octahedrally co-ordinated rocksalt structure at a modest pressure ($p \sim 0.4$ GPa [36]) whilst the Cu^+ co-ordination in CuI is lower than six up to the highest pressures measured ($p \sim 40$ GPa [37]). More direct evidence would be provided by molecular dynamics simulations which probe the nature of the conduction pathways at the microscopic level. However, on a more cautious note, such studies of the binary compound α-CuI have recently provided conflicting conclusions concerning the occupancy of the octahedral positions [38, 39].

In their classification scheme, Boyce and Huberman [6] labelled superionic compounds 'type I' if they show an abrupt superionic transition (i.e. a large jump in ionic conductivity associated with a first-order structural phase transition, as in AgI). Type II' superionic materials show a gradual increase in ionic conductivity arising from a gradual but anomalous increase in thermally induced lattice disorder (as in β-PbF_2). Amongst the superionic compounds, Ag_2HgI_4 and Cu_2HgI_4 are unusual because the transition to the highly conducting state is first order, with a large discontinuity in the ionic conductivity (see figure 2) but no reconstruction of the immobile anion sublattice. However, the structural behaviour of the 'parent' compound CuI on increasing temperature at elevated pressure shows similar behaviour, though the transition to the superionic state occurs via two first-order transitions and involves the presence of a partially disordered rhombohedral phase (CuI-IV), albeit with only a minor distortion of the f.c.c. I^- sublattice [40]. In the case of the ternary compounds, the abrupt nature of the transition has been explained by the migration of Ag^+/Cu^+ occurring between tetrahedral sites via the

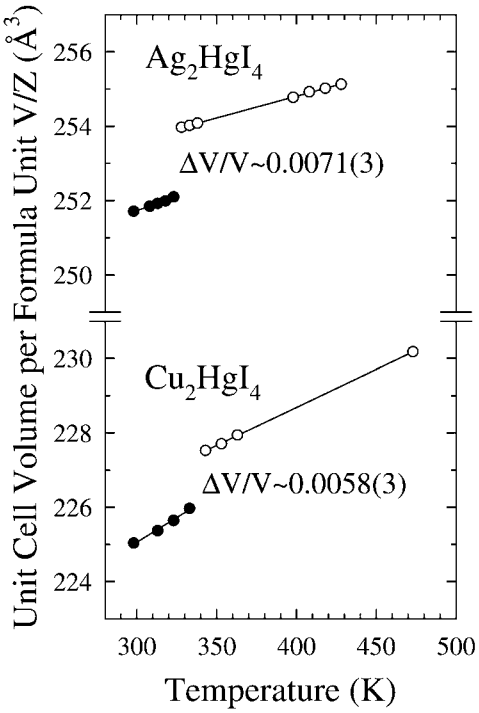

Figure 8. The variation of the unit cell volume per formula unit with temperature for Ag_2HgI_4 and Cu_2HgI_4 illustrating the volume changes at the superionic $\beta \rightarrow \alpha$ transitions.

octahedral ones [41]. Whilst in the octahedral sites, the monovalent cation would be near an Hg^{2+} and, therefore, energetically unfavourable. As a result, Ag^+/Cu^+ migration cannot occur until the Hg^{2+} have sufficiently large thermal vibrations to leave their regular sites and the divalent species can be considered to act as a 'valve' for the onset of superionic behaviour [41].

A number of previous studies have identified two transitions in Ag_2HgI_4 in the temperature region around 300 K [27, 42–44], suggesting that the structural and superionic transitions occur at slightly different temperatures. No such behaviour is observed in this work. Indeed, later measurements of stoichiometric samples showed only a single, abrupt $\beta \rightarrow \alpha$ transition, with the pre-transition behaviour due to the presence of an excess of AgI [45]. Similarly, we observe no evidence of a 'kink' in the ionic conductivity of α-Cu_2HgI_4 at ∼370 K as observed in one previous study and taken as the onset of Hg^{2+} motion [46]. The magnitudes of the volume change at the $\beta \rightarrow \alpha$ transitions are 0.0071(3) and 0.0058(3) for Ag_2HgI_4 and Cu_2HgI_4, respectively. These values are in good accord with those measured previously by dilatometer methods [43]. However, as illustrated in figure 8, there is no evidence of negative thermal expansion within α-Cu_2HgI_4 in the vicinity of the superionic transition as reported by Shibata *et al* [15]. Finally it is noted that there exist further, higher temperature stable phases of Ag_2HgI_4 and Cu_2HgI_4, at least one of which has a b.c.c. arrangement of anions. Further work is in progress to determine the structures of these, as yet uncharacterized, phases [47].

6. Conclusions

Clearly, it would be advantageous to investigate more isostructural Ag^+/Cu^+ superionic phases to determine why Ag^+ based compounds generally possess higher values of their ionic

conductivity. Possible examples are b.c.c. structured tellurides γ-Ag_2Te [48] and ε–Cu_2Te [49] and the b.c.c. structured iodides α–AgI and CuI-VII [40]. However, such measurements would be difficult owing to the extreme sensitivity of the conductivity to the exact stoichiometry (especially in the case of chalcogenides) and the need to perform experiments at elevated pressures and temperatures to reach the stability field of CuI-VII. Nevertheless, the quest for solid state batteries based on Cu^+ superionics provides a motivation, as the cost of Ag^+ based devices remains prohibitive, despite the promising electrochemical performance of compounds such as Ag_4RbI_5 [50].

Acknowledgments

We are grateful to N J G Gardner for assistance with the low temperature impedance spectroscopy measurements. The work presented in here forms part of a wider project investigating the structural properties of superionic conductors funded by the Engineering and Physical Sciences Research Council (reference GR/M38711).

References

[1] Chandra S 1981 *Superionic Solids. Principles and Applications* (Amsterdam: North-Holland)
[2] Wright A F and Fender B E F 1977 *J. Phys. C: Solid State Phys.* **10** 2261
[3] Bührer W and Hälg W 1977 *Electrochim. Acta* **22** 701
[4] Hoshino S, Sakuma T and Fujii Y 1979 *J. Phys. Soc. Japan* **47** 1252–9
[5] Geller S 1967 *Science* **157** 310–12
[6] Boyce J B and Huberman B A 1979 *Phys. Rep.* **51** 189
[7] Sukeshini A M and Hariharan K 1991 *Solid State Commun.* **78** 85
[8] Friesel M, Baranowski B and Lundén A 1990 *J. Phys. Chem.* **94** 1113
[9] Sudharsanan R and Clayman B P 1985 *Solid State Ion.* **15** 287
[10] Brodersen K, Göhr H and Schrenk J 1992 *Z. Naturforsch.* B **47** 17
[11] Wong T, Brodwin M, Shriver D F and McOmber J I 1981 *Solid State Ion.* **3/4** 53
[12] Leute V and Rusche H 1981 *J. Phys. Chem. Solids* **42** 303
[13] Slade R C T and Singh N 1992 *Solid State Ion.* **58** 9
[14] Becker S and Schön G 1984 *Solid State Ion.* **13** 141
[15] Shibata S, Hoshino H and Shimoji M 1974 *J. Chem. Soc. Faraday Trans.* I **70** 1409
[16] Burley G 1967 *Acta Crystallogr.* **23** 1
[17] Ketelaar J A A 1931 *Z. Kristallogr.* **80** 190
[18] Hahn H, Frank G and Klingler W 1955 *Z. Anorg. Allg. Chem.* **279** 271
[19] Brownall K W, Kasper J S and Wiedemeier H 1974 *J. Solid State Chem.* **10** 20
[20] Berthold H J and Kaese P M 1989 *Z. Kristallogr.* **186** 40
[21] Ketelaar J A A 1934 *Z. Kristallogr.* **87** 436
[22] Kasper J S and Browall K W 1975 *J. Solid State Chem.* **13** 49
[23] Hibma T, Beyeler H U and Zeller H R 1976 *J. Phys. C: Solid State Phys.* **9** 1691
[24] Armstrong R D, Bulmer R S and Dickinson T 1973 *J. Solid State Chem.* **8** 219
[25] Eriksson L, Wang P and Werner P-E 1991 *Z. Kristallogr.* **197** 235
[26] Gardner N J G, Hull S, Keen D A and Berastegui P 1998 *Rutherford Appleton Laboratory Report*, RAL-TR-1998-032
[27] Paic M and Paic V 1984 *Solid State Ion.* **14** 187
[28] Paic M and Paic V 1996 *Phase Transitions* **56** 11
[29] Hull S, Smith R I, David W I F, Hannon A C, Mayers J and Cywinski R 1992 *Physica* B **180/181** 1000
[30] David W I F, Ibberson R M and Matthewman J C 1992 *Rutherford Appleton Laboratory Report* RAL-92-032
[31] Brown P J and Matthewman J C 1987 *Rutherford Appleton Laboratory Report* RAL-87-010
[32] Sears V F 1992 *Neutron News* **3** 26
[33] Keen D A and Hull S 1994 *J. Phys.: Condens. Matter* **6** 1637
[34] Shannon R D 1976 *Acta Crystallogr.* A **32** 751
[35] Phillips J C 1970 *Rev. Mod. Phys.* **42** 317
[36] Keen D A and Hull S 1993 *J. Phys.: Condens. Matter* **5** 23

[37] Hofmann M, Hull S and Keen D A 1995 *Phys. Rev.* B **51** 12 022
[38] Ihata K and Okazaki H 1997 *J. Phys.: Condens. Matter* **9** 1477–92
[39] Zheng-Johansson J X M, Ebbsjö I and McGreevy R L 1996 *Solid State Ion.* **83** 35
[40] Hull S, Keen D A, Hayes W and Gardner N J G 1998 *J. Phys.: Condens. Matter* **10** 10 941
[41] LeDuc H G and Coleman L B 1985 *Phys. Rev.* B **31** 933
[42] Baranowski B, Friesel M and Lundén A 1983 *Solid State Ion.* **9/10** 1179
[43] Lumsden M, Steinitz M and McAlduff E J 1995 *J. Appl. Phys.* **77** 6039
[44] Friesel M, Baranowski B and Lundén A 1987 *Phys. Scr.* **35** 34
[45] Mellander B-E and Friesel M 1987 *Phys. Rev.* B **35** 7902
[46] Srivatava O P, Srivastava A K and Lal H B 1985 *J. Mater. Sci.* **20** 1763
[47] Keen D A and Hull S 1999 private communication
[48] Schneider J and Schulz H 1993 *Z. Kristallogr.* **203** 1
[49] Vouroutzis N and Manolikas C 1989 *Phys. Status Solidi* A **111** 491
[50] Owens B B and Bottelberghe J R 1993 *Solid State Ion.* **62** 243